GEOSCIENCES

Positive SAM trend as seen in the Brazilian Earth System Model (BESM) future scenarios

LUCIANA F. PRADO, ILANA WAINER & RONALD B. DE SOUZA

Abstract: Polar regions are among the most affected areas by the current global warming. In the Southern Hemisphere (SH), impacts of a warmer climate include decrease in sea-ice extent, changes in oceanic and in atmospheric circulation. Recently, some of these impacts were reinforced by the positive phase of the Southern Annular Mode (SAM). SAM is the dominant mode of variability of the SH extratropical climate and manifests as a "ring-shape" regular pattern of atmospheric mean sea level pressure (MSLP) with opposite sign between mid and high SH latitudes. Over the last three decades, SAM has presented a positive trend, and some studies associate it to stratospheric ozone depletion and to an increase in greenhouse gases concentration. As this debate is still open, climate models constitute useful tools to understand the SH variability in future scenarios. Here we use monthly MSLP outputs from the Brazilian Earth System Model (BESM) to examine SAM temporal and spatial behavior in future climate scenarios compared to the historical period. Our results for the BESM simulations suggest that the mean spatial pattern of SAM does not change with global warming, but an increase in the radiative forcing may reinforce positive SAM values obtained for the historical period.

Key words: Antarctica, CMIP5, Historical, mean sea level pressure, modes of variability, RCP.

INTRODUCTION

Global warming causes diverse impacts on Earth's climate system, and polar regions are among the most affected areas. In the Southern Hemisphere (SH), Antarctic sea-ice extent has decreased at a rate of 2% per decade over the period 1979-2015 (Comiso et al. 2017) with minimum records occurring in 2017 and 2018 (National Snow and Ice Data Center 2019). Future projections estimate a loss of one half of Antarctica's sea-ice cover by 2100 (Collins et al. 2013).

Recent studies suggest that under a 1.5 °C warming scenario, the number of days with surface air temperatures above 0 °C will increase, as well as the iceberg production, and changes in water masses characteristics are also projected (Siegert et al. 2019). Changes in the atmospheric circulation in the mid-to-high latitudes of the SH due to global warming are also suggested (Vaughan et al. 2003, Clem et al. 2020, Saurral et al. 2020). The warming of 0.61 ± 0.34 °C per decade over the last 30 years caused an intense cyclonic anomaly in the atmosphere at the Weddell Sea region that advected warm and moist air into Antarctica from the South Atlantic (Clem et al. 2020). This anomalous atmospheric circulation pattern was reinforced by the positive phase of the Southern Annular Mode (SAM, Rogers & van Loon 1982, Thompson & Wallace 2000).

SAM is the dominant mode of variability of the SH extratropical climate (Zheng et al. 2013), responsible for 22-34% of the SH atmospheric circulation variance (Gong & Wang 1999, Fogt & Marshall 2020), and for 10% of the variance of global atmospheric mass transport (Trenberth et al. 2005). SAM can be represented by a "ring-shape" regular pattern of atmospheric pressure at the 500 hPa geopotential height or mean sea level pressure (MSLP) anomalies with opposite signals between mid and high SH latitudes, representing its positive and negative phases. During positive SAM, negative MSLP anomalies occur above 60 °S and positive MSLP anomalies occur below 60 °S, resulting in stronger circumpolar westerlies, increased cyclone activity and stronger zonal winds (Russell & McGregor 2010). Negative SAM corresponds to the opposite pattern, with positive MSLP anomalies above 60 °S and negative MSLP anomalies in midlatitudes.

Over the last 30 years, SAM has presented a positive trend that could not be related to natural variability (Abram et al. 2014, McLandress et al. 2011). The stratospheric ozone depletion is suggested as the major forcing mechanism for this persistent positive trend (e.g., Fogt et al. 2017), reinforced by the increase in greenhouse gases' (GHG) concentrations as an effect of global warming (e.g., Arblaster & Meehl 2006). These two mechanisms alter the stratosphere-troposphere interactions and characteristics of the polar jet, resulting in a predominance of SAM's positive phase.

Aiming to understand future impacts of global warming, the International Panel on Climate Change (IPCC) recommended the use of specific scenarios to be applied to climate models with varying boundary conditions depending on projected radiative forcing. The Representative Concentration Pathways (RCPs, Moss et al. 2010) are characterized by conditions on the radiative forcing to be achieved by the end of the 21st century. The protocols for RCPs were developed by the Coupled Modeling Intercomparison Project phase 5 (CMIP5, Taylor et al. 2012) and made available for the scientific community.

The Brazilian initiative for the CMIP5 project is led by the Brazilian National Institute for Space Research (INPE) with the land-ocean-atmosphere coupled Brazilian Earth System Model (BESM) version OA2.5 (BESM-OA2.5, Nobre et al. 2013, Giarolla et al. 2015). In this study, we examine SAM trend in future scenarios using BESM-OA2.5 outputs. We compare two RCP scenarios with the historical (1850-2005) scenario by computing SAM indexes using MSLP anomalies. In this way, we aim to detect and quantify the observed positive SAM trend in BESM-OA2.5 outputs.

MATERIALS AND METHODS

We used MSLP monthly outputs from BESM-OA2.5 (Nobre et al. 2013, Giarolla et al. 2015). BESM-OA2.5 has been set up and run at INPE. The model uses the Flexible Modeling System (FMS) coupler from the Geophysical Fluid Dynamics Laboratory (GFDL) of the National Oceanic and Atmospheric Administration (NOAA). The atmospheric component of BESM-OA2.5 is the Brazilian Global Atmosphere Model (BAM, Figueroa et al. 2016) with horizontal resolution of ~ 1.875°, and 28 σ levels in the vertical. The oceanic component is the Modular Ocean Model version 4p1 (MOM4p1, Griffies 2009) with zonal resolution of 1°, meridional resolution from 0.25° to 2°, and 50 vertical levels. BESM-OA2.5 also includes the Sea Ice Simulator (SIS) ice model (Winton 2000).

In this study, we used BESM-OA2.5 monthly outputs from the CMIP5 historical experiment

(01/1850-12/2005)(Taylor et al. 2012) as the control experiment in order to examine future scenarios defined by RCP4.5 and RCP8.5 experiments (Moss et al. 2010). Only these two future scenarios were made available by INPE. Veiga et al. (2019) describe how these experiments were run in BESM-OA2.5. In the historical experiment, BESM-OA2.5 was forced by the atmospheric equivalent of historical CO_2 concentration, from January/1850 to December/2005. The RCP experiments are defined by changes in the radiative forcing in the year 2100 (relative to preindustrial conditions). For example, in the RCP4.5 (RCP8.5), the radiative forcing increases along time until reaching 4.5 W m^{-2} (8.5 W m^{-2}) in the year 2100 (Taylor et al. 2012).

For the SAM analysis, we computed the GW99 SAM index (Gong & Wang 1999) from BESM-OA2.5 monthly outputs from the historical, RCP4.5, and RCP8.5 experiments. The GW99 SAM index is defined as the difference of MSLP normalized monthly anomalies between 40 °S (P$^{*}_{40°S}$) and 65 °S (P$^{*}_{65°S}$) latitudinal belts:

$$SAM = P^{*}_{40°S} - P^{*}_{65°S} \tag{1}$$

A 10-yr moving average was applied to SAM index time series to allow examination of long-term variability. The unfiltered MSLP time series were converted into MSLP anomaly maps in order to represent the SAM spatial pattern in each analyzed experiment. SAM phases were examined by composing the MSLP anomaly field in months where SAM unfiltered index exceeded |2| standard deviations (SAM ≥ +2 standard deviation for SAM's positive phase; M ≤ -2 standard deviation for SAM's negative phase).

RESULTS

Mean fields of MSLP in the SH (20 °S to 90 °S) were examined for the all three experiments described earlier on in this text (Figure 1). We first compared the historical mean (Figure 1a) with the differences between the RCP scenarios and the historical mean (Figures 1b and 1c). The historical mean field (Figure 1a) showed a higher MSLP in SH midlatitudes (≥ 1013 hPa) whilst in latitudes higher than 60 °S the mean field presented MSLP ≤ 1013 hPa over the Southern Ocean, with the lowest values located in the eastern Southern Ocean. Over the Antarctic continent, however, MSLP values were higher again, with maximum MSLP in the eastern side. When comparing the RCP4.5 MSLP mean field with the historical (Figure 1b), we observe positive differences in midlatitudes (40 °S to 60 °S) and negative differences in latitudes higher than 60 °S. The same spatial pattern is observed for the difference between RCP8.5 and the historical experiment (Figure 1c), but the differences presented were higher, mainly over the Antarctic continent and the eastern regions of the Southern Ocean. The MSLP spatial pattern observed in RCP4.5 and RCP8.5 differences in respect to the historical experiment resembled the SAM's positive phase as seen in MSLP anomalies.

In order to describe the temporal variability of the MSLP, we used the measure of the standard deviation of the series. The historical MSLP standard deviation (Figure 1d) is higher over the continents in midlatitudes. The maximum values were observed over eastern Antarctica. A decrease in the standard deviation is noticeable in latitudes higher than 50 °S in both RCP4.5 and RCP8.5 scenarios (Figures 1e and 1f). An exception occurs in the eastern region of the Southern Ocean and over Australia.

We computed the 10-yr moving average of GW99 SAM index for the historical and RCP4.5 and RCP8.5 experiments (Figure 2) aiming to examine long-term variability and changes in the studied periods. The historical reconstruction of SAM
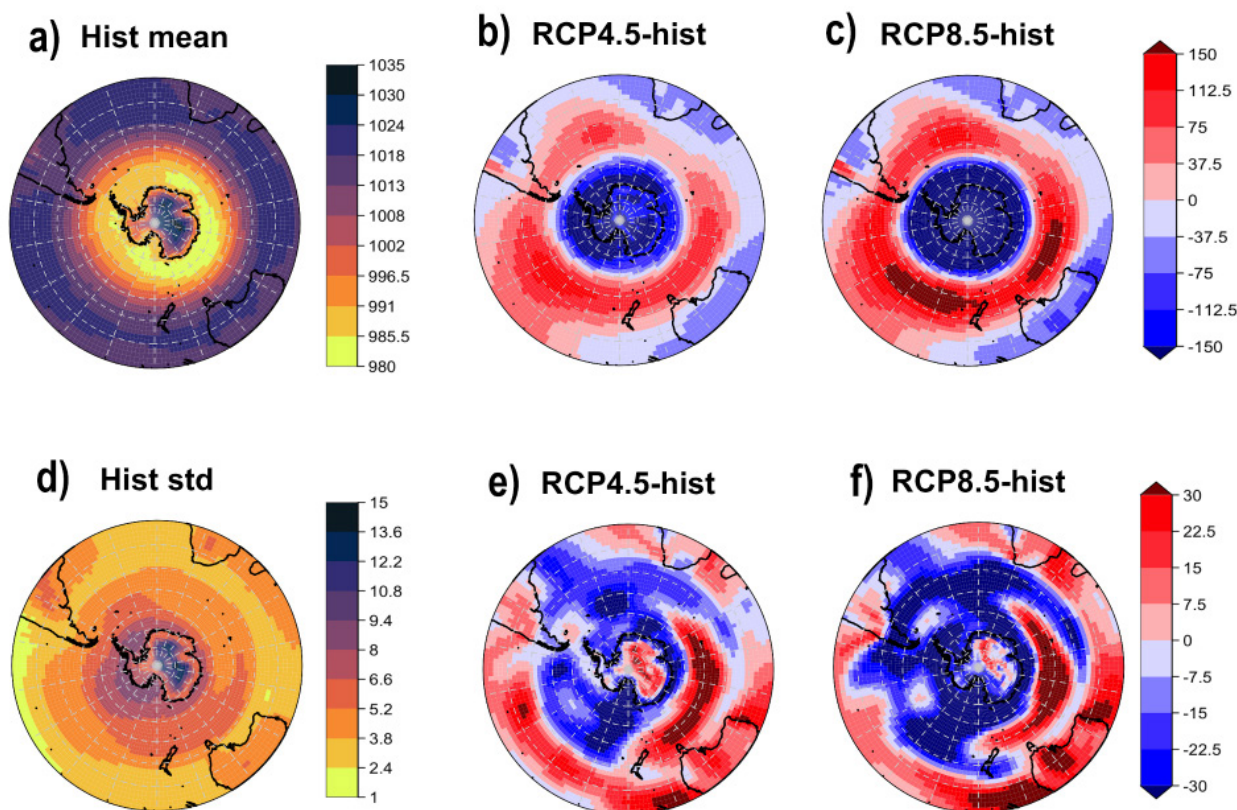
Figure 1. Mean sea level pressure in BESM-OA2.5 outputs: a) Historical mean (1850-2005); b) RCP4.5 and historical mean difference; c) RCP8.5 and historical mean difference; d) Historical mean variability; e) RCP4.5 and historical mean difference in variability; and f) RCP8.5 and historical mean difference in variability.

index (Figure 2a, purple line) showed periods when SAM's positive phase predominated (1890-1920; 1930's; 1960s; 1980-present), and others when the SAM's negative phase predominated (1860-1890;1920's; 1930-1970; 1970's). The magnitude of the SAM standardized index did not exceed +0.5 standard deviation for the positive SAM, and was between about -0.7 and zero for the negative SAM. A positive trend was observed for both RCPs' computed indexes (Figure 2b), although more remarkable in RCP8.5 (Figure 2b, red line). The extreme positive values of SAM index indicated that the maximum positive was equal to one standard deviation for RCP8.5 by the end of the century (Figure 2b, red line), but does not exceed 0.5 standard deviation for RCP4.5 (Figure 2b, blue line). For negative SAM, the minimum of -1 standard

deviation was observed for RCP4.5 (Figure 2b, blue line). RCP4.5 (Figure 2b, blue line) showed an alternation between positive and negative SAM indexes throughout time. RCP8.5 (Figure 2b, red line) SAM indexes were always positive from 2060 until the end of the 21st century. An out-of-phase relationship was observed between SAM indexes for RCP4.5 and RCP8.5.

In order to examine how BESM-OA2.5 outputs were able to reproduce SAM's spatial pattern in each experiment, we regressed the unfiltered GW99 SAM time series onto MSLP anomalies field (Figure 3). Historical (Figure 3a), RCP4.5 (Figure 3b), and RCP8.5 (Figure 3c) regressions present a similar MSLP spatial pattern, with negative correlations at high latitudes (higher than 60 °S) and positive correlations at midlatitudes (lower than 60 °S).
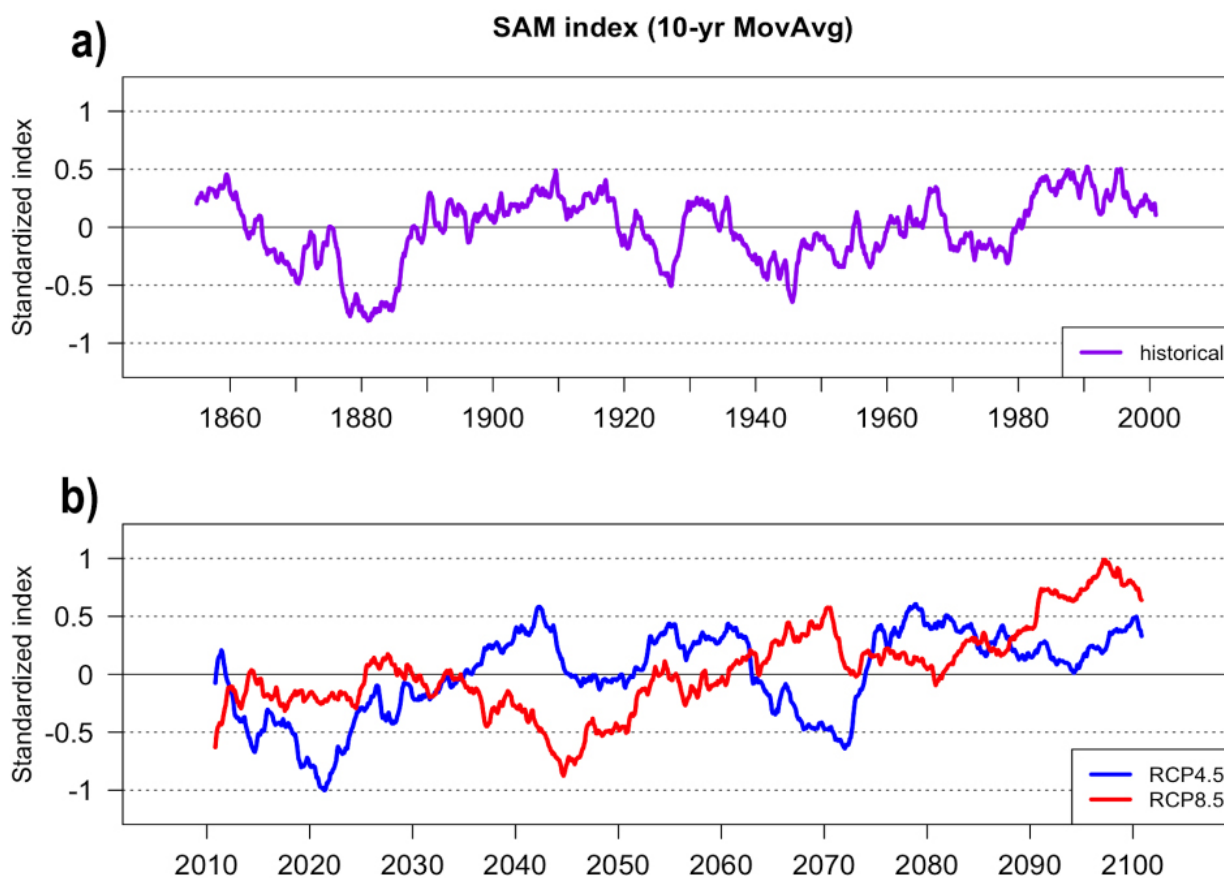
Figure 2. GW99 10-yr moving average of SAM index in BESM-OA2.5: a) Historical (purple line); b) RCP4.5 (blue line), and RCP8.5 (red line).

SAM's characteristic annular shape was clearly present in all three experiments investigated here, but the magnitude of correlation varied among the experiments.

MSLP anomalies were composited into SAM positive and negative phases for the three experiments examined here (Figure 4). The positive phase of SAM (Figures 4a, 4b and 4c) was characterized by negative MSLP anomalies in latitudes higher than 60 °S, and positive MSLP anomalies at midlatitudes. Highest positive MSLP anomalies were observed in the Australian sector of the Southern Ocean, and the lowest negative MSLP anomalies occurred over the Antarctic continent. No differences in the spatial structure of SAM positive phase were observed among the experiments, except for a decrease in

magnitude in the positive belt associated with the increase of the radiative forcing in the RCP scenarios.

The negative phase of SAM (Figures 4d, 4e, and 4f) resulted in positive MSLP anomalies over Antarctica and the Southern Ocean reaching 60 °S, and negative MSLP anomalies in latitudes lower than 60 °S, with the minimum at about 45 °S. The annular structure of the MSLP anomalies was clear, with lowest negative anomalies occurring in the eastern Southern Ocean. SAM negative pattern presented no changes in its spatial structure or in the MSLP anomalies' magnitudes among the examined experiments.
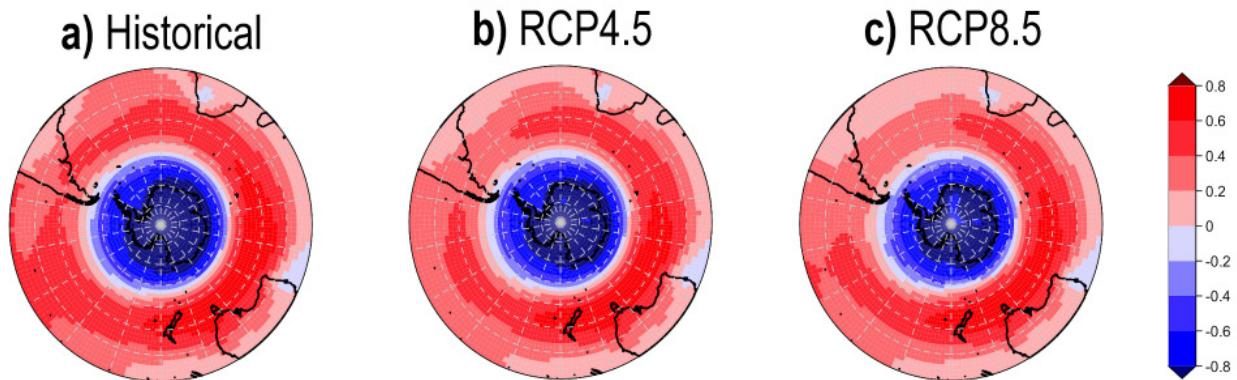
Figure 3. GW99 SAM index regressed onto SLP monthly anomalies. a) Historical, b) RCP4.5, and c) RCP8.5. Values correspond to the correlation coefficient and are nondimensional.
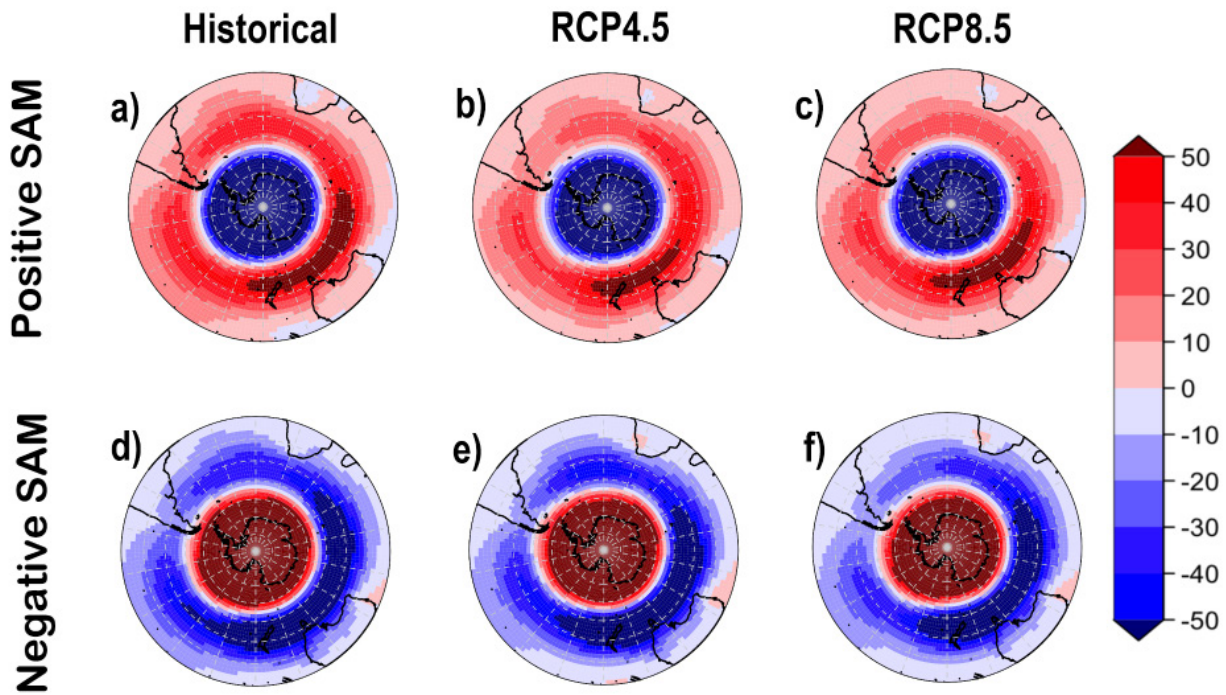

Figure 4. SAM positive and negative phases SLP composites for a) and d) Historical, b) and e) RCP4.5, and c) and f) RCP8.5. Composites were obtained for MSLP anomalies exceeding |2| standard deviation in the SAM index time series.

DISCUSSION

SAM variability is related to changes in the extratropical atmospheric circulation from the Earth's surface to the stratosphere, and is influenced by changes in the tropical sea surface temperature (SST) variability (Fogt & Marshall 2020). The position and intensity of the polar jet changes along the year, influenced by SST variability, and alters the atmospheric circulation in midlatitudes. During the positive phase of SAM, positive zonal wind anomalies intensify the polar jet that shifts poleward (Kidson & Sinclair 1995). Zonal mean air temperatures are affected by the changes in the polar jet, resulting in a tropospheric adiabatic

cooling (warming) in the southern (northern) side of the polar jet. The opposite occurs during the negative phase of SAM (Fogt & Marshall 2020). These changes impact the strength of the Ferrel and Hadley circulation (e.g., Thompson & Wallace 2000) and the eddy momentum flux of the atmosphere (Limpasuvan & Hartmann 1999) and, consequently, the planet's climate at lower latitudes. As SAM is also influenced by the tropical SST variability, the El Niño - Southern Oscillation (ENSO) phases (positive – El Niño, negative – La Niña) impact the polarity of the SAM via Rossby waves, resulting in changes in the location and intensity of the polar jet (Fogt et al. 2011).

During the austral winter, the meridional air temperature gradient between polar and tropical latitudes is enhanced as the insolation decreases towards Antarctica. That strengthens the polar vortex and the circumpolar stratospheric westerly winds (Hurrell et al. 1998). As the air temperature increases during the austral spring, the stratosphere-troposphere interactions are favored by the polar vortex breakdown due to the weakening of stratospheric winds (Fogt & Marshall 2020). This relationship between troposphere and stratosphere circulation anomalies mediates the impact of stratospheric ozone changes in SAM's variability.

Recent studies detected a positive trend in SAM along the last 30 years that could not be attributed to natural variability when compared to long-term estimates and model simulations (Abram et al. 2014, McLandress et al. 2011). Many studies suggest the stratospheric ozone depletion as a primary mechanism driving this positive trend in SAM (Thompson & Solomon 2002, Polvani et al. 2011, Fogt et al. 2017) because of the temperature-related troposphere-stratosphere interaction. The positive trend is detected mainly during austral summer, because of the lower troposphere response time

to perturbations in stratosphere (Thompson & Solomon 2002). A positive trend in sea surface height (SSH) was also detected in the SH for BESM-OA2.5 and other CMIP5 models for RCP4.5 and RCP8.5 future scenarios, as a result of the thermal expansion of the oceans in the upper 700 m due to global warming (Giarolla et al. 2020).

In spite of the primary influence of stratospheric ozone on positive SAM trend during austral summer, the increase in greenhouse gases (GHG) concentrations along the last decades would amplify the trend during the other seasons. The ozone effect would be reinforced by GHG-related warming of the troposphere and the cooling of the stratosphere, resulting in an amplification of the pole-to-equator air temperature gradient and an enhancement of the circumpolar westerly winds, that favors the positive SAM (e.g., Arblaster & Meehl 2006). Moreover, Marshall et al. (2004) suggest that the observed positive SAM trend is associated with a non-linear interaction between natural and anthropogenic forcing, because the trend initiated 10 years before the ozone loss by the SH stratosphere.

Our results with BESM-OA2.5 outputs showed the predominance of the SAM's positive phase since 1980 in the historical experiment, although not presenting a positive trend. The historical warming trend is not clear in BESM-OA2.5 historical run. A possible cause for that is because BESM-OA2.5 does not include aerosols processes in opposition to other CMIP5 models (Veiga et al. 2019). In RCP4.5 and RCP8.5 experiments, however, the positive SAM trend increased with the radiative forcing, presenting maximum positive SAM index values by the end of the 21st century in the RCP8.5 scenario. Differences between RCP scenarios and the historical mean MSLP also reveal a prevalence of the SAM positive phase for warmer (RCP)

scenarios. These results corroborate previous findings, as they show a preference of the SAM positive phase to be present in the mean MSLP fields of warmer future scenarios. SAM's positive phase is also seen in the long-term monthly index time series of the historical and the forced experiments. This suggests a SAM response to both the ozone forcing by the end of the historical period as well as to the global warming represented by the RCP scenarios.

Veiga et al. (2019) also examined SAM in BESM-OA2.5 historical run. Contrary to the present work, the authors applied EOF analysis to monthly mean 500 hPa geopotential height from 1950 to 2005 and compared their fields to NOAA-20Cv2 reanalysis. Their results show differences in the amplitude of signals between BESM-OA2.5 and reanalysis, but SAM's spatial patterns were similar.

Other recent studies have investigated impacts of an increase in atmospheric CO_2 in the climate system using BESM-OA2.5 simulations. By comparing BESM-OA2.5 results with CMIP5 models for the abrupt $4xCO_2$ protocol, Capistrano et al. (2020) examined responses of temperature, precipitation, atmospheric circulation and radiative feedback, showing that BESM-OA2.5 performance is within the ensemble mean spread, except for a strong positive cloud feedback. Using the same outputs but including CMIP6 models, Casagrande et al. (2020) obtained evidences of seasonality in the polar amplification response related to sea ice changes in the abrupt $4xCO_2$ scenario.

CONCLUSIONS

Here we explored the spatial and temporal characteristics of the Southern Annular Mode (SAM) in BESM-OA2.5 results for the CMIP5 historical and future scenarios experiments,

using monthly MSLP fields. BESM-OA2.5 was able to reproduce the spatial structure of both positive and negative SAM phases which did not present significant changes among the examined experiments.

Our findings showed a predominance of the positive phase of SAM since the 1980's until the end of the historical period. The positive trend in future scenarios was intensified by the increase in radiative forcing in BESM-OA2.5 RCP4.5 to RCP8.5 experiments. These results corroborate previous studies that associate the SAM positive trend to the global warming and to the stratospheric ozone depletion. BESM-OA2.5 is able reproduce the SAM pattern and its future trends, offering a reliable, in house option for climate studies in the Southern Hemisphere.

REFERENCES

ABRAM NJ, MULVANEY R, VIMEUX F, PHIPPS SJ, TURNER J & ENGLAND MH. 2014. Evolution of the Southern Annular Mode during the past millennium. Nat Clim Change 4(7): 564-569.

ARBLASTER JM & MEEHL GA. 2006. Contributions of external forcings to southern annular mode trends. J Climate 19(12): 2896-2905.

CAPISTRANO VB ET AL. 2020. Assessing the performance of climate change simulation results from BESM-OA2.5

compared with a CMIP5 model ensemble. Geosci Model Dev 13: 2277-2296.

CASAGRANDE F, SOUZA RB, NOBRE P & MARQUEZ AL. 2020. Na inter-hemispheric seasonal comparison of polar amplification using radiative forcing of a quadrupling CO2 experiment. Ann Geophys 38: 1123-1138.

CLEM KR, FOGT RL, TURNER J, LINTNER BR, MARSHALL GJ, MILLER, JR & RENWICK A. 2020. Record warming at the South Pole during the past three decades. Nat Clim Change 10: 762-770.

COLLINS M ET AL. 2013. Long-term climate change: projections, commitments and irreversibility. In Climate Change 2013-The Physical Science Basis: Contribution of Working Group I to the Fifth Assessment Report of the Intergovernmental Panel on Climate Change. Cambridge University Press, 1029-1136.

COMISO JC, GERSTEN RA, STOCK LV, TURNER J, PEREZ GJ & CHO K. 2017. Positive trend in the Antarctic sea ice cover and associated changes in surface temperature. J Climate 30(6): 2251-2267.

FIGUEROA SN ET AL. 2016. The Brazilian Global Atmospheric Model (BAM): Performance for Tropical Rainfall Forecasting and Sensitivity to Convective Scheme and Horizontal Resolution. Weather Forecast 31: 1547-1572.

FOGT RL, BROMWICH DH & HINES KM. 2011. Understanding the SAM influence on the South Pacific ENSO teleconnection. Clim Dynam 36(7-8): 1555-1576.

FOGT RL, GOERGENS CA, JONES JM, SCHNEIDER DP, NICOLAS JP, BROMWICH DH & DUSSELIER HE. 2017. A twentieth century perspective on summer Antarctic pressure change and variability and contributions from tropical SSTs and ozone depletion. Geophys Res Lett 44(19): 9918-9927.

FOGT RL & MARSHALL GJ. 2020. The Southern Annular Mode: variability, trends, and climate impacts across the Southern Hemisphere. WIREs Cli Change 11: e652.

GIAROLLA E, SIQUEIRA LSP, BOTTINO MJ, MALAGUTTI M, CAPISTRANO VB & NOBRE P. 2015. Equatorial Atlantic Ocean dynamics in a coupled ocean atmosphere model simulation. Ocean Dynam 65: 831-843.

GIAROLLA E, VEIGA SF, NOBRE P, SILVA JR MB, CAPISTRANO VB & CALLEGARE AO. 2020. Sea surface height trends in the southern hemisphere oceans simulated by the Brazilian Earth System Model under RCP4.5 and RCP8.5 scenarios. J South Hemisp Earth Syst Sci 70: 280-289.

GONG D & WANG S. 1999. Definition of Antarctic oscillation index, Geophys Res Lett 26: 459-462.

GRIFFIES SM. 2009. Elements of MOM4p1. NOAA/Geophysical Fluid Dynamics Laboratory Ocean Group Tech Rep 6: 444 p.

HURRELL JW, VAN LOON H & SHEA DJ. 1998. The mean state of the troposphere. In: KAROLY DJ & VINCENT DG (Eds), Meteorology of the southern hemisphere. Boston, MA: American Meteorological Society, 1-46.

KIDSON JW & SINCLAIR MR. 1995. The influence of persistent anomalies on Southern Hemisphere storm tracks. J Climate 8(8): 1938-1950.

LIMPASUVAN V & HARTMANN DL. 1999. Eddies and the annular modes of climate variability. Geophys Res Lett 26(20): 3133-3136.

MARSHALL GJ, STOTT PA, TURNER J, CONNOLLEY WM, KING JC & LACHLAN-COPE TA. 2004. Causes of exceptional atmospheric circulation changes in the Southern Hemisphere. Geophys Res Lett 31: L14205.

MCLANDRESS C, SHEPHERD TG, SCINOCCA JF, PLUMMER DA, SIGMOND M, JONSSON AI & READER MC. 2011. Separating the dynamical effects of climate change and ozone depletion. Part II: Southern Hemisphere troposphere. J Climate 24(6): 1850-1868.

MOSS RH ET AL. 2010. The next generation of scenarios for climate change research and assessment. Nature 463(7282): 747-756.

NATIONAL SNOW AND ICE DATA CENTER. 2019. All about sea ice, accessed on Apr 01st 2021, https://nsidc.org/data/seaice_index/.

NOBRE P ET AL. 2013. Climate simulation and change in the Brazilian climate model. J Climate 26: 6716-6732.

POLVANI LM, WAUGH DW, CORREA GJP & SON S-W. 2011. Stratospheric ozone depletion: The main driver of twentieth-century atmospheric circulation changes in the Southern Hemisphere. J Climate 24(3): 795-812.

ROGERS JC & VAN LOON H. 1982. Spatial variability of sea level pressure and 500 mb height anomalies over the Southern Hemisphere. Mon Weather Rev 110(10): 1375-1392.

RUSSELL A & MCGREGOR GR. 2010. Southern hemisphere atmospheric circulation: impacts on Antarctic climate and reconstructions from Antarctic ice core data. Clim Change 99: 155-195.

SAURRAL RI, RAGGIO GA & GULIZIA CN. 2020. How could a difference of 0.5° C in global warming modify the mean and extreme climate conditions around Antarctica?. Int J Climatol 40(14): 6067-6079.

SIEGERT M ET AL. 2019. The Antarctic Peninsula under a 1.5 C global warming scenario. Front Environ Sci 7: 102.

TAYLOR KE, STOUFFER RJ & MEEHL GA. 2012. An overview of CMIP5 and the experiment design. Bull Am Meteorol Soc 93(4): 485-498.

THOMPSON DWJ & SOLOMON S. 2002. Interpretation of recent Southern Hemisphere climate change. Science 296(5569): 895-899.

THOMPSON DWJ & WALLACE JM. 2000. Annular modes in the extratropical circulation. Part I: Month-to-month variability. J Clim 13(5): 1000-1016.

TRENBERTH KE, STEPANIAK DP & SMITH L. 2005. Interannual variability of the patterns of atmospheric mass distribution. J Climate 18: 2812-2825.

VAUGHAN DG, MARSHALL GJ, CONNOLLEY WM, PARKINSON C, MULVANEY R, HODGSON DA, KING JC, PUDSEY CJ & TURNER J. 2003. Recent Rapid Regional Climate Warming on the Antarctic Peninsula. Clim Change 60: 243-274.

VEIGA SF ET AL. 2019. The Brazilian Earth System Model ocean-atmosphere (BESM-OA) version 2.5: evaluation of its CMIP5 historical simulation. Geosci Model Dev 12: 1613-1642.

WINTON M. 2000. A reformulated three-layer sea ice model. J Atmos Ocean Tech 17: 525-531.

ZHENG F, LI J, CLARK RT & NNAMCHI HC. 2013. Simulation and projection of the Southern Hemisphere annular mode in CMIP5 models. J Clim 26: 9860-9879.

How to cite

LUCIANA F. PRADO[1,2]
https://orcid.org/0000-0002-6446-8986

ILANA WAINER[1]
https://orcid.org/0000-0003-3784-623X

RONALD B. DE SOUZA[3]
https://orcid.org/0000-0003-3346-3370

[1]Universidade de São Paulo, Instituto Oceanográfico, Praça do Oceanográfico, 191, Cidade Universitária, 05508-120 São Paulo, SP, Brazil

[2]Universidade de Brasília, Instituto de Geociências, Instituto Central de Ciências, Campus Darcy Ribeiro, 70297-400 Brasília, DF, Brazil

[3]Instituto Nacional de Pesquisas Espaciais (INPE-CPTEC), Centro de Previsão de Tempo e Estudos Climáticos, Divisão de Modelagem Numérica do Sistema Terrestre,   Rodovia Presidente Dutra Km 40, 12630-000 Cachoeira Paulista, SP, Brazil

Correspondence to: **Luciana Figueiredo Prado**
E-mail: luciana.prado@usp.br

Author contributions

Study conception: LFP, IW, RBS; Data analyses: LFP; Manuscript main writing: LFP; Manuscript editing and review: LFP, IW, RBS.